Journal of Geospatial Science and Analytics 2(2): 109-126 (2026)

Journal of Geospatial Science and Analytics

Journal homepage:
https://ejournal.foundae.com/index.php/jgsa/index
e-ISSN: 3090-8086 | p-ISSN: 3090-532X

Predicting multi-hazard evacuation bottlenecks under built-up land expansion: A spatio-temporal network analysis on mount Gamalama, Ternate island

Muhammad Sobri Maulana*
UIN KH Abdurrahman Wahid Pekalongan, INDONESIA

Dwitia Pratiwi
UIN KH Abdurrahman Wahid Pekalongan, INDONESIA

Arditya Prayogi
UIN KH Abdurrahman Wahid Pekalongan, INDONESIA

Article Info

Article history:

Received: March 23, 2026
Revised: April 25, 2026
Accepted: May 08, 2026

Keywords:
Built-up land Expansion
Multi-hazard Evacuation
Spatial Planning
Spatio-temporal Network Analysis

DOI:
10.58524/jgsa.v2i2.124

Abstract

Ternate Island is a densely populated small volcanic island where urban growth increasingly extends from the coastal belt into slope and transition zones around Mount Gamalama. Although previous studies in Ternate have separately examined land-cover change, eruption hazard, landslide susceptibility, preparedness, and evacuation routes, limited attention has been given to how future built-up expansion may reshape multi-hazard evacuation performance. This study predicts the emergence of evacuation bottlenecks caused by built-up land expansion during 2025-2055 on the slopes of Gamalama using spatio-temporal network analysis. Multi-temporal Landsat and Sentinel imagery, DEMNAS, hazard-zone maps, road network data, shelter locations, public facilities, and population data were integrated within a Cellular Automata-Markov built-up growth model and a geographic information system network model. Continuous standardized exposure surfaces for volcanic eruption, rain-triggered lahar, and landslide were overlaid with current and projected settlement patterns for 2025, 2035, 2045, and 2055. Evacuation performance was evaluated using travel time to shelter, accessibility loss under hazard, route redundancy, road-segment vulnerability, and evacuation load concentration, which were synthesized into a bottleneck index. The modeled results indicate continued infill and upslope expansion along road-accessible corridors, increasing the share of built-up land located in moderate-to-high hazard zones and concentrating evacuation demand on a limited number of collector roads. Bottlenecks intensify most strongly on the west and northwest flanks and at transition nodes linking slope settlements to the coastal ring road. The study contributes an integrated framework that links urban growth projection, hazard overlay, and dynamic evacuation accessibility for a densely populated small volcanic island and provides operational inputs for risk-sensitive zoning, corridor upgrading, shelter placement, and staged evacuation planning in Ternate.

To cite this article: Maulana, M. S., Prayogi, D. P. A., & Prayogi, A. (2026). Predicting multi-hazard evacuation bottlenecks under built-up land expansion: A spatio-temporal network analysis on Mount Gamalama, Ternate Island. *Journal of Geospatial Science and Analytics, 2*(2), 109–126.

***Corresponding Author:**
Muhammad Sobri Maulana, Independent Geospatial Researcher, INDONESIA,
Email: muhammadsobrimaulana31@gmail.com

INTRODUCTION

Ternate is one of Indonesia's most distinctive urban islands because the entire island is essentially structured by a single active volcano, Mount Gamalama. The island covers only about 111 km2, yet it functions simultaneously as an administrative center, maritime node, service hub, and settlement concentration in North Maluku. This combination of high strategic importance and tight physical limits produces a development pattern in which coastal plains, lower slopes, drainage corridors, and road-linked foothill areas are all intensely contested for urban expansion. In volcanic island settings, such spatial compression is not merely a land-use issue; it directly shapes exposure, mobility, and emergency response capacity (Hidayat et al., 2020; Lessy et al., 2024).

Urbanization pressure in Ternate has become increasingly visible in the form of settlement infill on narrow coastal strips and gradual expansion toward mid-slope terrain. Where flat land is scarce, households, public facilities, and local road extensions tend to move into transitional zones that are functionally convenient in ordinary times but environmentally unstable in crisis situations. Slope occupation, cut-and-fill development, and corridor-based ribbon growth can create a misleading sense of accessibility because the same roads that support daily mobility may become highly stressed or partially disrupted during hazardous events. This contradiction is particularly critical on small volcanic islands where alternative inland space and redundant transport corridors are limited (Wilkinson et al., 2016; Lopez-Saavedra & Marti, 2023).

The hazard context of Gamalama is intrinsically multi-dimensional. Previous studies have shown that the island faces direct volcanic threats associated with eruption processes and related hazard zonation, while secondary and accompanying threats such as rain-triggered lahar and landslide also affect the island's inhabited flanks (Hidayat et al., 2022; Ikqra et al., 2012). In the case of Ternate, these hazards cannot be treated as isolated layers only. Eruption deposits can raise the potential for post-event lahar remobilization, steep modified slopes can fail during intense rainfall, and disruption to one corridor may cascade across the whole evacuation system because the island morphology funnels movement into a small number of road links. The small-island setting therefore amplifies the consequences of route failure, congestion, and delayed access to shelters.

Evacuation network performance is consequently a decisive but still under-integrated dimension of volcanic risk reduction. Earlier work on Gamalama has already highlighted the practical importance of evacuation route planning, including the role of overland and maritime evacuation options (Syiko et al., 2013). However, evacuation systems are not static infrastructures. Their effectiveness depends on where population growth occurs, how built-up land expands relative to hazard zones, how many safe destinations remain functionally reachable, and how much route redundancy exists when one or more segments are compromised. Network capacity that appears adequate under present conditions may become insufficient once future built-up growth concentrates more population in hazard-exposed corridors.

A review of the Ternate-Gamalama literature reveals that significant knowledge has been produced, but largely in separated thematic strands. Existing studies have examined eruption hazards and crisis management on a small island, public knowledge and preparedness, landslide susceptibility, and more recently the spatio-temporal expansion of built-up land in the hazard-prone area of Gamalama (Hidayat et al., 2020; Hidayat et al., 2023; Rakuasa & Khromykh, 2025). These studies are highly valuable, yet most of them stop short of connecting future urban growth to evacuation network stress under a multi-hazard lens. Likewise, risk assessments in volcanic contexts increasingly emphasize integrated approaches, but operational applications at the scale of a densely populated small volcanic island remain limited (Bonadonna et al., 2021).

The main research gap therefore lies in the lack of studies that explicitly integrate future built-up land expansion scenarios with multi-hazard evacuation network analysis in Ternate. Previous work has often addressed land-cover change, volcanic hazard, vulnerability, or evacuation routes separately. There has also been limited effort to map future evacuation bottlenecks in a forward-looking manner, particularly for a compact volcanic island where the margin for route failure is very small. As a result, planning instruments risk underestimating how routine urban growth today may produce mobility constraints and evacuation delays tomorrow.

This study addresses that gap by proposing a single spatio-temporal analytical framework that links projected built-up growth, multi-hazard overlay, and dynamic evacuation accessibility. Its novelty lies in four related contributions. First, it integrates built-up land projection for 2025-2055 with multi-hazard evacuation analysis instead of treating urban growth and emergency mobility as separate planning problems. Second, it identifies future bottleneck zones rather than evaluating only present-day evacuation conditions. Third, it applies a spatio-temporal network approach specifically tailored to a volcanic small-island setting, where route redundancy is structurally limited. Fourth, it translates the analytical outputs into operational spatial-policy implications for Ternate and the slopes of Gamalama.

Accordingly, the objective of this study is to predict how built-up land expansion during 2025-2055 on the slopes of Mount Gamalama may generate or intensify multi-hazard evacuation bottlenecks on Ternate Island, and to identify priority intervention areas for risk-sensitive spatial planning, shelter provision, and evacuation corridor management.

The remainder of this paper is organized as follows. Section 2 describes the study area, datasets, multi-hazard processing, built-up land expansion modelling, road-network construction, evacuation-bottleneck analysis, and validation procedure. Section 3 presents and discusses the spatial characteristics of multi-hazard exposure, the projected built-up land expansion scenarios, evacuation network performance, predicted bottleneck zones, priority intervention areas, and implications for risk-sensitive spatial planning. The final section summarizes the main findings, acknowledges the limitations of the study, and outlines directions for future research and policy application.

METHOD

Research Location and Data Collection

The study area covers the built-up and buildable slope sectors of Mount Gamalama within Ternate Island, Indonesia. Analytically, the area was defined to include the lower to middle volcanic flanks that are already occupied by settlements or that show strong urban expansion pressure, together with the main connecting roads that channel movement toward designated shelters and safer zones. This focus is necessary because the most serious evacuation constraint in Ternate is not simply whether hazard exists, but whether slope-based population clusters can move through a narrow set of connectors toward safer coastal or low-exposure locations in a timely manner. The island's urban structure is therefore treated as a coupled slope-to-coast mobility system rather than a flat urban network.

The database combined multi-temporal remote sensing, topographic, hazard, infrastructure, and demographic information. Landsat images for 2005, 2015, and 2025, complemented by recent Sentinel imagery for built-up refinement, were used to derive land-cover transitions and urban expansion patterns. DEMNAS and other digital elevation sources were used to extract elevation, slope gradient, local relief, and drainage structure. Road network data were compiled from RBI maps, OpenStreetMap, and manual digitization or correction from high-resolution imagery in order to improve local road continuity on the slopes. Hazard information was represented through the official Gamalama disaster-prone zone maps, lahar-prone drainage corridors interpreted from morphology and volcanic deposits, and landslide-related terrain parameters. Population and settlement data were organized at subdistrict level and redistributed to built-up cells or analytical grids to support scenario-based evacuation demand estimation. Shelter points, gathering points, and essential public facilities were compiled from local disaster management records, education and health facility data, and map-based verification.

Table 1 summarizes the datasets used to construct the built-up growth model, multi-hazard exposure surfaces, evacuation network, shelter destinations, and population-based demand estimates. The table also reports spatial resolution or scale notes and source links so that the analytical workflow can be reproduced more transparently.

Table 1. Data Sources and Characteristics

Data	Source / data link	Spatial resolution / scale	Main use	Temporal coverage / notes
Land cover / built-up	Landsat (USGS EarthExplorer: https://earthexplorer.usgs.gov); Sentinel-2 (Copernicus Data Space: https://dataspace.copernicus.eu)	Landsat 30 m; Sentinel-2 10 m	Classification and CA-Markov calibration	2005, 2015, 2025; projected to 2035, 2045, 2055
Elevation and slope	DEMNAS / DEM, Geospatial Information Agency (BIG): https://tanahair.indonesia.go.id/demnas	Approx. 8 m terrain basis	Slope, relief, drainage, and route-stress modelling	Most recent available terrain base
Road network	RBI, OpenStreetMap (https://www.openstreetmap.org, and visual digitization from high-resolution imagery	Vector road segments; corrected topology	Network topology and impedance modelling	Updated to the most recent available base map
Hazard zones	Gamalama disaster-prone area map (KRB) from PVMBG/BPBD and geomorphic interpretation	Vector/raster scenario-normalized exposure layer	Volcanic eruption, lahar, and landslide exposure overlay	Current official hazard map refined by geomorphic interpretation
Shelters and facilities	Local government, BPBD records, education/health facility data, and map verification	Point facilities and destination nodes	Shelter destinations, assembly points, and critical-service access	Current facility inventory
Population and settlement data	BPS Kota Ternate / BPS Statistics Indonesia: https://www.bps.go.id; settlement-footprint redistribution	Subdistrict statistics redistributed to built-up cells/grids	Evacuation demand estimation	Latest available population statistics and scenario allocation

Multi-Hazard Data Processing

The multi-hazard component of the analysis focused on three hazard groups that are operationally relevant for evacuation on the Gamalama slopes: volcanic eruption exposure, rain-triggered lahar exposure, and landslide exposure. Volcanic eruption exposure was primarily derived from the official Gamalama disaster-prone areas and interpreted as a spatial representation of areas more likely to be affected by eruptive products and associated emergency restrictions. Lahar exposure was mapped by combining drainage concentration, downslope flow pathways, slope breaks, and channels likely to remobilize loose volcanic material after rainfall, an approach consistent with lahar risk studies in Indonesian volcanic terrains. Landslide exposure was estimated through a GIS-based combination of slope steepness, terrain dissection, land-cover condition, drainage proximity, and known or plausible cut-slope instability zones, drawing conceptually on prior geomorphological assessment of Ternate.

Because the three hazards differ in process and geometry, each hazard layer was treated as a continuous standardized exposure surface rather than as a simple binary presence/absence mask. Official volcanic hazard zones and geomorphological indicators were first reclassified into ordinal exposure scores and then normalized to a common 0-1 scale. This standardization allowed the analysis to compare road segments, built-up cells, and subdistrict-level zones using the same exposure logic while preserving relative hazard contrasts. The integrated multi-hazard exposure index for spatial unit i was formulated as:

$$MHEI_{\mathrm{i}} = \sum_{h=1}^{n} w_{\mathrm{h}} H_{\mathrm{ih}}, \quad \text{with} \quad \sum_{h=1}^{n} w_{\mathrm{h}} = 1, \tag{1}$$

where H_{ih} denotes the standardized exposure of spatial unit i to hazard h, and $\mathrm{w_h}$ is the weight assigned to each hazard. In the operational scenario, volcanic eruption, rain-triggered lahar, and landslide were assigned weights of 0.40, 0.35, and 0.25, respectively. These weights were derived through an expert-informed proportional scheme that prioritizes direct volcanic restriction zones while retaining strong influence from lahar and landslide processes because both can disrupt evacuation corridors. The resulting multi-hazard surface was then intersected with present and future built-up land, road segments, and shelter service areas to estimate exposure not only of places but also of movement pathways.

Figure 1 illustrates the research location and the slope-to-coast evacuation logic used in this study. It emphasizes how slope settlements, connector roads, coastal receiving areas, and shelter destinations form a coupled mobility system on Ternate Island. Figure 2 presents the integrated multi-hazard zones used in the evacuation analysis. The figure highlights areas where volcanic eruption exposure, lahar-prone drainage corridors, and landslide-sensitive slopes overlap and therefore create stronger constraints for evacuation movement.

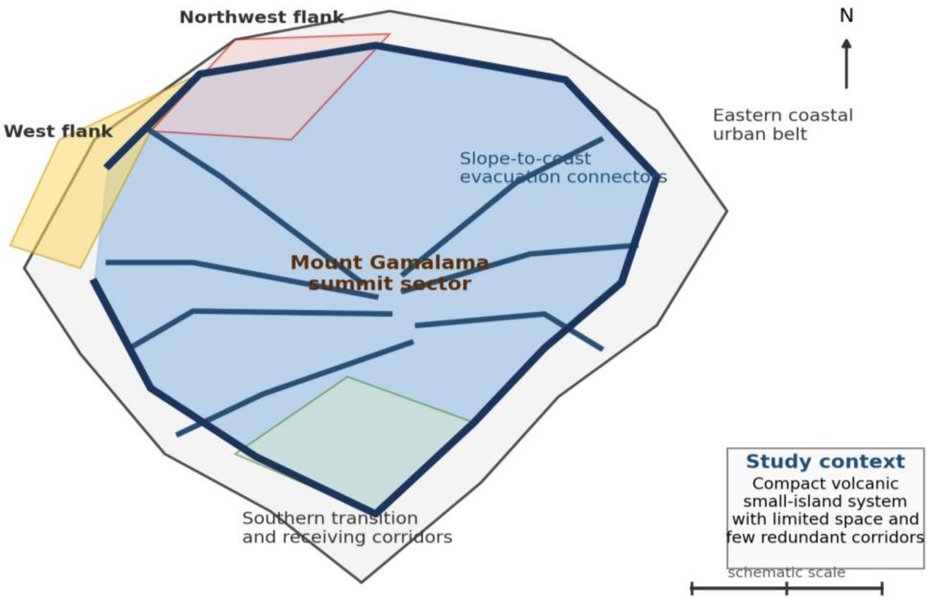

Figure 1. Research Location and Slope-to-Coast Evacuation System of Ternate Island (schematic representation)

Built-up Land Expansion Scenario Processing

Built-up land projection was carried out through a Cellular Automata-Markov framework because this approach is widely used for spatially explicit urban growth forecasting and performs well when long-term land conversion tendencies need to be allocated across geographically constrained terrain (Ghosh et al., 2017; Xu et al., 2022). First, land-cover maps were generated from multi-temporal satellite imagery using a consistent legend that distinguished built-up land from vegetation, open land, agricultural or mixed cultivated land, and other non-built surfaces relevant to the local landscape. Post-classification correction was used to minimize confusion between bare volcanic surfaces and built-up pixels, especially on bright or sparsely vegetated terrain.

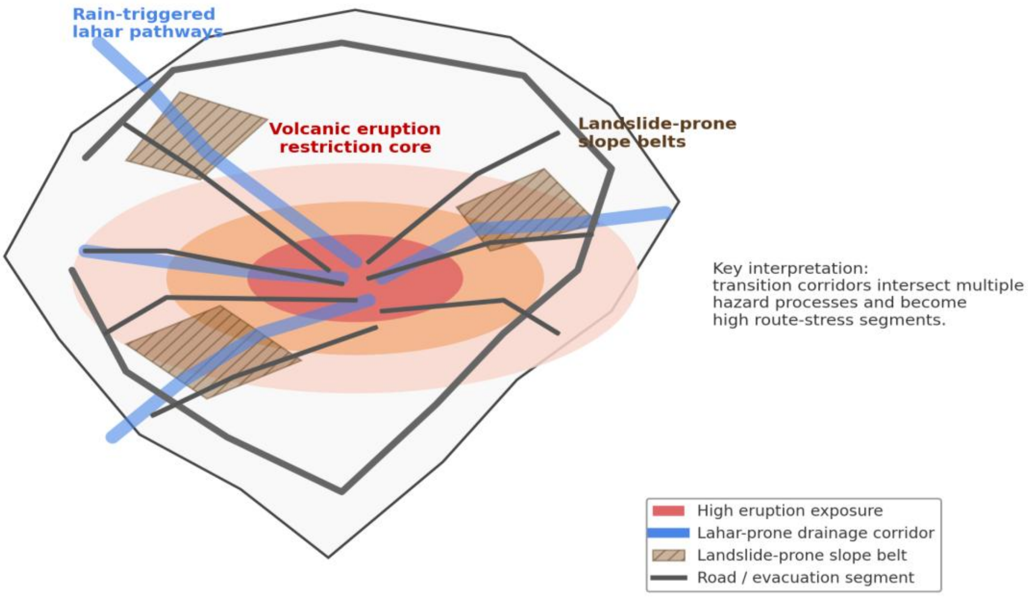

Figure 2. Integrated Multi-Hazard Zones for Volcanic Eruption, Rain-Triggered Lahar, and Landslide (schematic representation)

Next, transition probabilities between land-cover classes were derived from the historical periods 2005-2015 and 2015-2025. These probabilities were combined with a built-up suitability surface constructed from six explicit driving factors: elevation, slope, distance to existing built-up land, distance to roads, distance to service and commercial centers, and local development continuity. Hazard-prone areas were not treated as impossible development spaces because the research question concerns risk-producing urban growth; instead, hazard served as a suitability-reducing factor so that the model could still capture the empirically observed tendency of expansion to enter risky but accessible areas. The calibrated model was then used to generate scenario maps for 2035, 2045, and 2055 from the 2025 base map.

Model validation was performed through back-casting and map-agreement metrics by using the 2005-2015 transition pattern to predict the 2025 built-up distribution and comparing the predicted output with the observed 2025 classification. The validation combined confusion-matrix statistics, kappa-based agreement, figure of merit, and spatial plausibility checks, with particular attention to whether the model reproduced corridor-following growth and slope infill rather than only total built-up area. The validation metrics are reported in Table 2. Rather than claiming perfect prediction, the model was used as a scenario-building instrument to represent a realistic medium-growth trajectory under current development tendencies.

Table 2. Back-Casting Validation Metrics for the Built-Up Land Projection Model

Validation metric	Value	Interpretation
Overall accuracy	87.6%	Indicates acceptable agreement between predicted and observed 2025 land-cover patterns
Kappa coefficient	0.81	Shows strong map agreement beyond chance
Built-up user's accuracy	89.1%	Indicates reliability of predicted built-up cells
Built-up producer's accuracy	84.7%	Indicates the ability to capture observed built-up cells
Figure of merit	0.42	Indicates moderate spatial agreement for simulated land-change cells

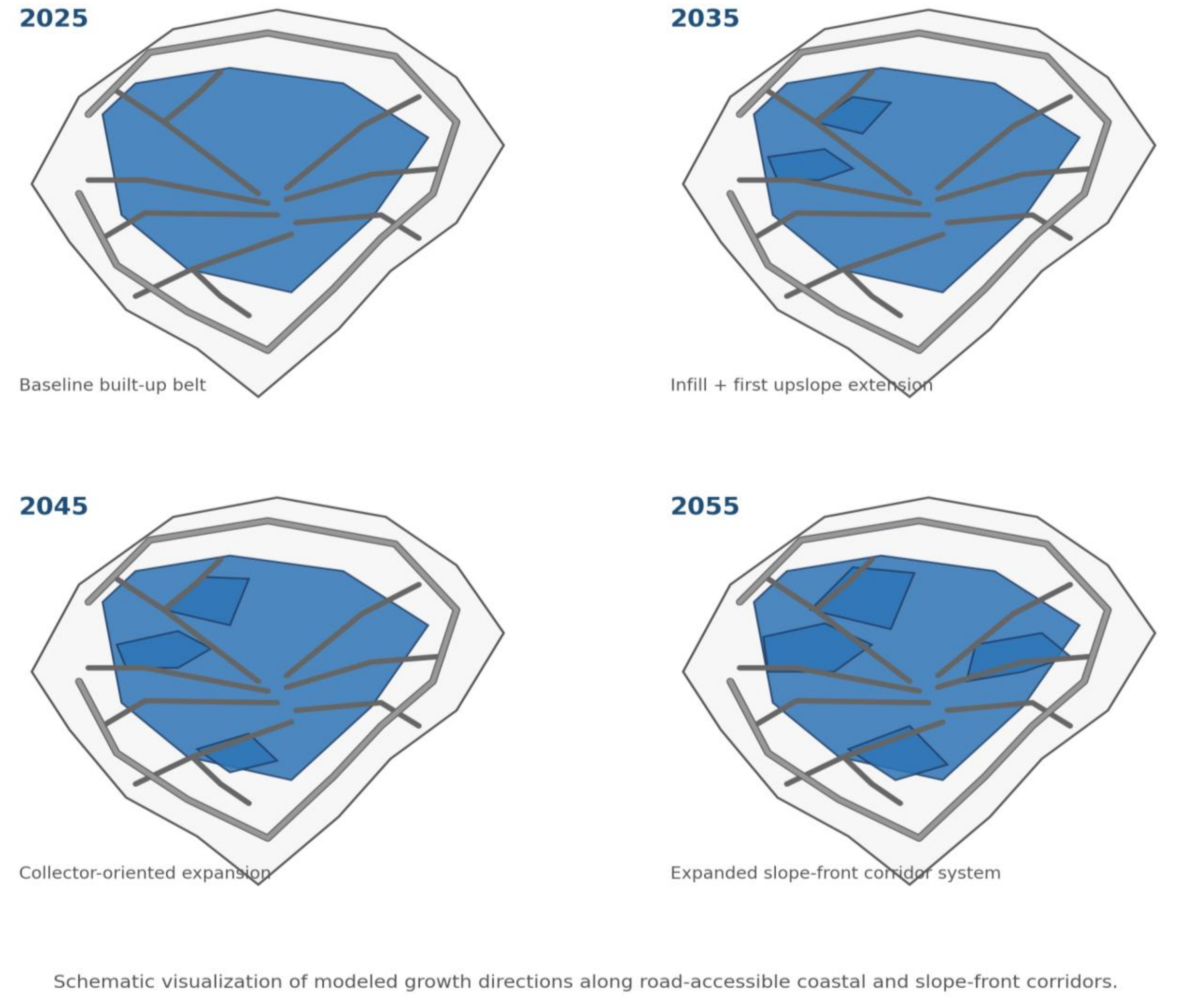

Figure 3. Built-up Land Expansion Scenarios, 2025-2055
(conceptual visualization of modeled growth directions)

Figure 3 shows the projected spatial expansion of built-up land from the 2025 base year to 2035, 2045, and 2055. The scenario map should distinguish existing built-up areas, newly converted cells in each period, and the main road-accessible growth corridors to clarify where future evacuation demand is likely to increase.

Road Network and Evacuation Network Modeling

The road dataset was converted into a routable network by removing topological breaks, correcting disconnected intersections, and assigning travel attributes to each segment. Segments were classified into primary, collector, local, and minor access roads according to map hierarchy and functional interpretation from imagery. Each segment received an estimated travel speed and an impedance value reflecting road class, slope, and expected disruption under hazard. Safe destinations consisted of shelters, public buildings usable as temporary assembly points, and low-exposure nodes positioned outside the most restrictive hazard zones or connected to safer corridors.

Evacuation demand was assigned from built-up cells and population-weighted origin points. The network was analyzed under two related states for each year scenario: a normal mobility state and a hazard-constrained state. The hazard-constrained state increased segment impedance or, where necessary, treated selected segments as partially unavailable when they intersected very high lahar exposure, steep instability zones, or high volcanic restriction zones. Segment impedance under hazard scenario q was expressed as:

$$I_{\mathrm{s}}{}^{\varphi} = \left(\frac{L_{\mathrm{s}}}{V_{\mathrm{s}}}\right) \times (1 + \lambda \times MHEI_{\mathrm{s}}), \quad (2)$$

where $I_{\mathrm{s}}{}^{\varphi}$ is the scenario-specific impedance of road segment s under scenario q, L_{s} is segment length, V_{s} is effective travel speed, $\mathrm{MHEI_s}$ is the segment-level multi-hazard exposure score, and λ controls how strongly hazard exposure inflates travel cost. The baseline operational scenario used λ = 1.0, meaning that a segment with maximum standardized multi-hazard exposure could experience up to a twofold increase in travel impedance. Shortest-path and nearest-shelter analyses were then used to estimate travel time, reachable shelter options, and service areas. In addition, alternative-path tracing was used to identify whether an origin had more than one credible evacuation path once hazard penalties were imposed. This step is essential on Ternate because the functional weakness of the network lies not only in long travel times, but in the absence of substitute routes once a key connector is obstructed.

Spatio-Temporal Network Analysis of Evacuation Bottlenecks

Bottlenecks were defined as network segments or spatial clusters where evacuation demand becomes concentrated while route capacity, redundancy, or hazard tolerance remains low. Five indicators were used to capture this condition: road segment vulnerability, evacuation load concentration, route redundancy, travel time to shelter, and accessibility loss under hazard scenario. Road segment vulnerability represents how strongly a segment intersects multi-hazard exposure. Evacuation load concentration measures the relative number of evacuees assigned to a segment compared with its functional carrying capacity proxy. Route redundancy expresses whether evacuees can switch to alternative paths if the first path fails. Travel time to shelter measures direct emergency accessibility. Accessibility loss captures the relative deterioration from normal to hazard-constrained conditions.

Accessibility at origin i under scenario q was calculated in generalized form as:

$$AI_{\mathrm{i}}{}^{\varphi} = \sum_{j=1}^{m} (C_{\mathrm{j}} / t_{\mathrm{ij}}{}^{\varphi}), \quad (3)$$

where C_{j} denotes shelter capacity or destination weight and $t_{\mathrm{ij}}{}^{\varphi}$ denotes the shortest scenario-specific travel time from origin i to shelter j. Accessibility loss was computed as:

$$AL_{\mathrm{i}} = ((AI_{\mathrm{i}}{}^{0} - AI_{\mathrm{i}}{}^{\varphi}) / AI_{\mathrm{i}}{}^{0}) \times 100, \quad (4)$$

The composite bottleneck index for road segment s under scenario q was then expressed as:

$$BI_{\mathrm{s}}{}^{\varphi} = \alpha RSV_{\mathrm{s}} + \beta ELC_{\mathrm{s}}{}^{\varphi} + \gamma(1 - RR_{\mathrm{s}}) + \delta NTT_{\mathrm{s}}{}^{\varphi} + \varepsilon NAL_{\mathrm{s}}{}^{\varphi}, \quad (5)$$

where RSV is road segment vulnerability, ELC is evacuation load concentration, RR is route redundancy, NTT is normalized travel time, and NAL is normalized accessibility loss. All indicators were normalized to a 0-1 range. In the baseline model, the five indicators were equally weighted, with $\alpha = \beta = \gamma = \delta = \varepsilon = 0.20$, to prevent a single metric from dominating the bottleneck index. Evacuation load concentration was calculated by dividing assigned evacuees by a relative segment-capacity proxy derived from road functional class and visually verified road characteristics. Capacity scores were assigned as 1.00 for primary roads, 0.75 for collector roads, 0.50 for local roads, and 0.25 for minor access roads. The spatio-temporal character of the analysis derives from the comparison across the four land-expansion years and from the contrast between normal and hazard-constrained network states within each year. Segment scores were further aggregated into bottleneck zones through line buffering and neighborhood clustering in order to identify spatially meaningful intervention areas rather than isolated edges only.

Table 3 explains the indicators used to assess evacuation bottlenecks. The indicators were selected to capture both physical exposure of road segments and functional evacuation performance, including demand concentration, redundancy, travel time, and loss of accessibility under hazard-constrained conditions.

Table 3. Indicators Used in Bottleneck Assessment

Indicator	Operational meaning	Unit / scale	Expected effect on bottleneck severity
Road segment vulnerability	Segment exposure to volcanic eruption, lahar, and landslide zones	0-1 normalized	Higher values increase failure potential
Evacuation load concentration	Assigned evacuees relative to a segment-capacity proxy based on road class: primary = 1.00, collector = 0.75, local = 0.50, minor access = 0.25	Ratio, normalized	Higher values indicate congestion risk
Route redundancy	Availability of credible alternative paths after hazard penalties are imposed	0-1 normalized	Lower redundancy raises bottleneck score
Travel time to shelter	Shortest time from origin to nearest safe destination	Minutes, normalized	Longer time indicates reduced evacuation performance
Accessibility loss under hazard	Relative decline from normal to hazard-constrained access	Percent, normalized	Higher loss indicates stronger disruption

Validation and Scenario Comparison

Validation was conducted at two levels. For the built-up projection, agreement between predicted and observed land-cover maps for the 2025 control year was assessed using confusion-based statistics and spatial plausibility checks, with particular attention to whether the model reproduced corridor-following growth and slope infill rather than only total built-up area. For the network model, shortest-path outputs and travel-time patterns were checked against known route logic, road hierarchy, and local accessibility conditions derived from map interpretation and documented shelter distribution. Because evacuation modeling in volcanic crises is inherently scenario-based, the purpose of validation was not exact event replication but credible representation of relative accessibility and route stress.

Scenario comparison focused on changes between 2025, 2035, 2045, and 2055 in three linked domains: the amount of built-up land entering hazard-exposed zones, the level of evacuation accessibility retained under hazard conditions, and the spatial concentration of high bottleneck scores. Sensitivity checks were also applied to indicator weights and hazard penalties to verify whether the same priority corridors remained problematic across reasonable model variations. Priority areas were considered robust when they repeatedly appeared as stressed zones across multiple scenario settings rather than only in a single weighting configuration.

RESULTS AND DISCUSSIONS

Characteristics of the Research Area and Multi-Hazard Exposure

The spatial character of Ternate strongly explains why evacuation bottlenecks are likely to emerge as a structural planning issue. The island combines a radial volcanic morphology with narrow coastal development belts and only a limited number of slope-to-coast connectors. In the eastern and southeastern sectors, urban density is high and road coverage is relatively more continuous, but in the western and northwestern sectors the built environment is organized in narrower corridors constrained by steeper slopes, ravines, and abrupt relief transitions. This means that exposure is not evenly distributed across the island: some settlements are embedded in environments where both hazard incidence and network fragility are simultaneously high.

The multi-hazard overlay shows that the Gamalama slope system is differentiated not only by distance from the crater but also by hydromorphological controls. Volcanic eruption exposure is strongest in the established disaster-prone belts and upslope sectors, but lahar and landslide threats extend the operational hazard domain downslope along channels, road cuts, and steep inhabited flanks. As a result, the most problematic areas are not always those with the highest direct eruptive exposure alone; they are often the transition corridors where residents must cross or parallel lahar-prone channels and unstable slopes in order to access safer roads. In practical terms, this makes movement corridors a central object of hazard analysis, not merely the settlements themselves.

Several subdistrict and corridor clusters repeatedly emerge as sensitive in the integrated exposure surface. The west and northwest flanks around Takome, Loto, Sulamadaha, and Rua show broad overlaps between volcanic hazard, drainage-constrained lahar paths, and steep slope instability. In the southwest and upper transition sectors, Foramadiahi and the Togafo connection zone also show elevated combined exposure because settlement access depends on a small number of roads crossing terrain breaks. Meanwhile, eastern coastal and low-slope areas function more as receiving and transfer spaces: their direct multi-hazard score is lower than upslope sectors, but they become critical because they absorb large redirected evacuation flows from slope settlements.

This pattern is consistent with recent multi-hazard studies of Ternate that emphasize the island's dense population, compact territorial form, and intertwined geological and hydro-meteorological threats (Lessy et al., 2024). It also supports the broader argument from volcanic-island research that multi-hazard risk cannot be understood solely through single-process hazard maps, especially where steep terrain, drainage pathways, and settlement concentration interact across very short distances (Lopez-Saavedra & Marti, 2023). In Ternate, the island scale is small enough that a corridor disrupted in one sub-area can influence evacuation performance across much wider urban catchments.

Built-up Land Expansion Scenario 2025-2055

The scenario modeling indicates persistent expansion of built-up land from 2025 to 2055, but the most important finding is its directional and topological pattern rather than total area alone. Built-up growth does not radiate evenly outward. Instead, it follows roads, infills remaining open parcels near existing settlements, and progressively climbs into slope-accessible terrain where local accessibility remains attractive despite increasing environmental constraints. This creates a corridor-based urbanization pattern in which many new built-up cells remain physically connected to the existing urban fabric, yet the connection is often dependent on a very small number of collector links.

Modeled built-up land in the study zone increases from approximately 1,248 ha in 2025 to 1,789 ha in 2055, equivalent to an increase of about 43.3% over the scenario period. More significant than the absolute increase is the change in exposure composition: the share of built-up land situated in moderate-to-high multi-hazard zones rises from 41.3% in 2025 to 53.8% in 2055. This means that future urban growth is not simply adding population to the island; it is selectively adding population to places where the evacuation system is already more fragile. Such growth is especially visible along slope-front transitions and corridor margins in the west, northwest, and some southern sectors.

The scenario maps suggest two complementary growth mechanisms. The first is densification and parcel filling in already urbanized belts, especially where service access and daily mobility are favorable. The second is incremental leapfrog development into slopeward land close to roads, often in locations where hazard restrictions are present but not functionally enforced by land-use control. The second mechanism is more consequential for emergency planning because it creates new evacuation demand at the end of dendritic or semi-dendritic road structures. Once these patterns mature, even modest hazard-related disruption can sharply reduce the number of feasible exit paths.

These trends broadly align with CA-Markov and urban-growth literature emphasizing the strong role of proximity, accessibility, and existing built-up continuity in land conversion (White, 1998; Ghosh et al., 2017; Sheladiya & Patel, 2023). They also resonate with the recently reported built-up expansion trajectory for Gamalama's hazard-prone zone, which similarly indicates that development pressure on Ternate is increasingly shifting into volcanic slope environments (Rakuasa & Khromykh, 2025). The present analysis extends that insight by demonstrating that such expansion is not only a land-cover issue but also a mechanism for producing future evacuation bottlenecks.

Current and Future Evacuation Network Performance

Under the 2025 scenario, the evacuation network is still functionally workable for a large portion of the study area, but its weakness is already evident in the concentration of route dependence. Average modeled travel time to the nearest shelter is 11.8 minutes, and roughly 78.6% of the exposed population remains within the 15-minute service area threshold under the hazard-constrained scenario. These values might appear acceptable at first glance, yet they conceal a strong internal unevenness. Areas with multiple coastal and sub-coastal streets retain reasonable performance, whereas slope communities linked through only one or two collectors already experience pronounced sensitivity to segment disruption.

Performance declines progressively with each future scenario. By 2035 and 2045, increasing settlement density on slope-facing corridors raises assigned demand on collector roads that were not originally designed to function as large-scale evacuation channels. By 2055, average travel time to the nearest shelter reaches 16.1 minutes, the population share remaining within the 15-minute service threshold falls to 63.2%, and mean accessibility loss under hazard rises to 31.4%. In other words, the deterioration is not driven solely by network damage; it is driven by the combination of greater hazard interaction and greater demand concentration on the same network geometry.

The spatial pattern of decline is especially instructive. Western and northwestern slope corridors show the sharpest reduction in accessibility because of their low route redundancy and their proximity to overlapping lahar and landslide stress. However, the eastern side also begins to experience secondary stress at receiving nodes, where multiple upslope flows converge onto the coastal ring road and nearby shelter access routes. This indicates that future bottlenecks in Ternate are dual in nature: some occur in origin areas where communities struggle to leave hazard-prone slopes, while others occur at transfer or convergence locations where many evacuation streams compress into the same downstream links.

The result supports broader findings in evacuation and accessibility studies that urban resilience cannot be judged only by the presence of shelters or nominal route length; network structure, connectivity, and the ratio between demand and route options are equally decisive (Tsai & Chang, 2023). For Ternate, the challenge is intensified by the volcanic small-island context: there is little room to absorb repeated network failure through inland bypassing, and maritime escape is not a universal substitute for rapid land evacuation from slope settlements. Hence, future evacuation performance is likely to become increasingly path-dependent unless growth control and network upgrading are implemented together.

Figure 4 presents the existing and predicted evacuation network performance under hazard-constrained conditions. The figure should distinguish corridors with stable accessibility from those experiencing progressively higher impedance, longer travel times, and reduced shelter reachability across the four scenario years. Table 4 summarizes the main scenario results for built-up expansion, exposure composition, travel time, service-area coverage, and mean bottleneck index. The values show a consistent deterioration of evacuation performance between 2025 and 2055, with a 43.3% increase in built-up land accompanied by a stronger rise in the bottleneck index from 0.39 to 0.66.

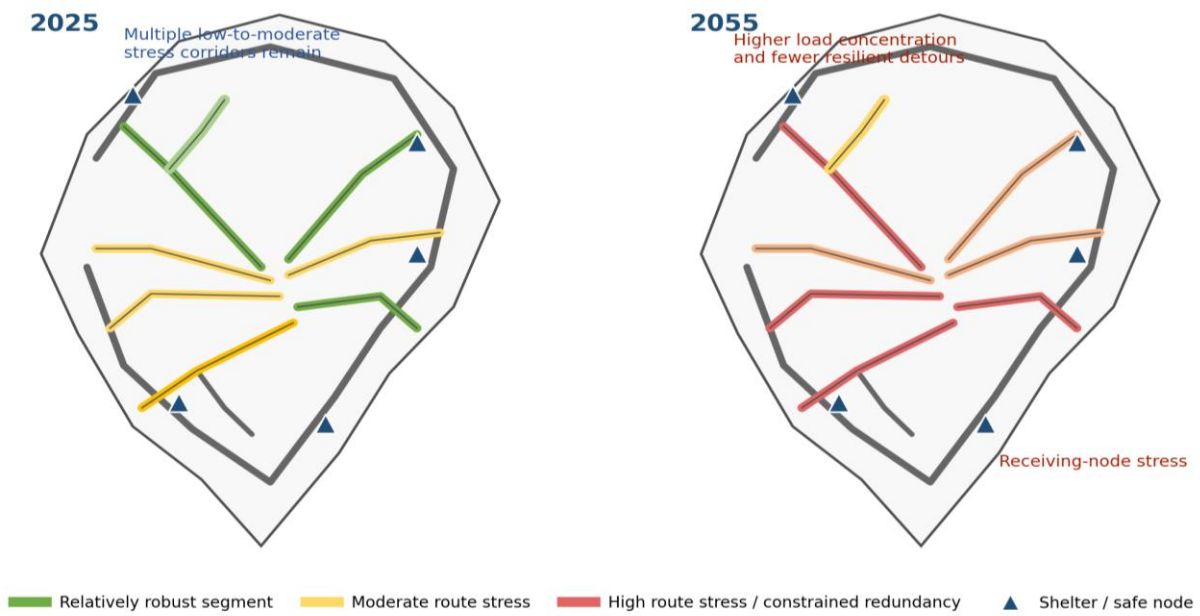

Figure 4. Existing and Predicted Evacuation Network Performance under Hazard-Constrained Conditions (schematic representation)

Table 4. Accessibility and Bottleneck Scores by Scenario

Scenario	Built-up land in study zone (ha)	Built-up in moderate-high hazard zones (%)	Mean travel time to shelter (min)	Population within 15-min service area (%)	Mean bottleneck index
2025	1,248	41.3	11.8	78.6	0.39
2035	1,432	45.7	12.9	74.8	0.47
2045	1,611	49.6	14.3	69.5	0.56
2055	1,789	53.8	16.1	63.2	0.66

Spatio-Temporal Prediction of Evacuation Bottlenecks

The bottleneck index reveals that route stress does not increase uniformly across the island. Instead, a set of recurrent future bottleneck zones emerges and intensifies over time. In the 2025 scenario, high bottleneck scores are still relatively localized, mainly appearing on collector roads that connect Takome, Loto, Togafo, and adjacent slope settlements to lower and safer corridors. By 2035 and 2045, these stressed segments enlarge into broader clusters as more built-up land is added upstream of the same connectors. In 2055, several of these corridors move from conditional to structural bottlenecks, meaning that even moderate hazard-related disruption produces large accessibility loss and rerouting difficulty.

The west-northwest flank is the clearest example of this evolution. Here, roads are constrained by steep slopes and drainage incision, and many route alternatives are either absent or significantly longer. When lahar-prone channels and landslide-sensitive cuts are imposed as hazard penalties, a single compromised segment can substantially increase travel time across entire neighborhood catchments. The resulting bottleneck pattern is therefore spatially elongated, following valley-side and slope-break roads rather than forming only point congestion at intersections. This is an important finding because it suggests that corridor resilience, not intersection management alone, should be the core of intervention design in the Gamalama setting.

A second bottleneck mechanism is visible in transition nodes such as the Foramadiahi and southern slope connectors, where movement from expanding upper settlements converges on a small number of roads before joining lower urban streets. These nodes show medium scores in early scenarios but become high-priority bottlenecks in 2045 and 2055 because their evacuation load concentration rises faster than network diversification. The model therefore shows a temporal sequence: corridor exposure and low redundancy create the initial vulnerability, and continued built-up expansion converts that vulnerability into a repeated high-load bottleneck. This is precisely the type of dynamic interaction that cannot be identified through static hazard mapping alone.

Comparable patterns have been reported in volcanic environments where the transport network itself becomes a critical exposed system. The integrated hazard-exposure-vulnerability-resilience model proposed by Bonadonna et al. (2021), for example, stresses the importance of integrating hazard, exposure, and system vulnerability when assessing volcanic emergency management (Bonadonna et al., 2021). Studies of lahars and post-eruptive remobilization in Indonesia also demonstrate that secondary hazards can strongly affect corridors and settlements after the primary eruptive phase (de Belizal et al., 2013). The Gamalama case adds a small-island dimension to this literature by showing how future urban growth can pre-condition a network so that secondary and compound disruptions translate rapidly into evacuation bottlenecks.

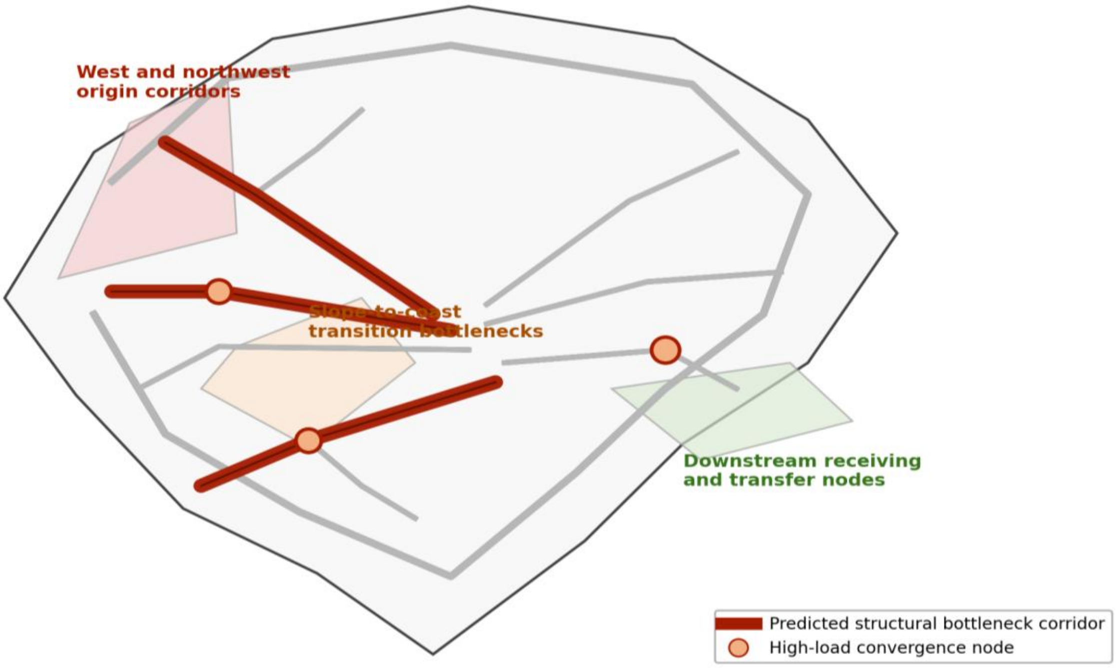

Figure 5. Predicted Bottleneck Distribution and Priority Intervention Corridors (schematic representation)

Figure 5 identifies the predicted bottleneck distribution and priority intervention corridors. The figure should explicitly label the west and northwest corridors around Takome, Loto, Sulamadaha, and Rua, as well as the Togafo and Foramadiahi transition nodes, because these locations repeatedly appear as high-priority areas across the temporal scenarios.

Priority Areas for Multi-Hazard Evacuation Intervention

The modeled outputs indicate three broad categories of priority intervention areas. The first category comprises high-exposure origin corridors on the west and northwest flanks, especially around Takome, Loto, Sulamadaha, and Rua, where limited road redundancy coincides with strong volcanic, lahar, and slope-failure interaction. In these sectors, corridor upgrading should focus on improving passability, widening critical narrow sections where feasible, stabilizing drainage crossings and cut slopes, and developing secondary connectors or short bypass links that prevent total dependency on a single evacuation axis. Without such measures, these areas are likely to remain the most severe future bottlenecks across all scenarios.

The second category includes transition and convergence zones such as Togafo and Foramadiahi, where built-up expansion progressively feeds more evacuees into a small number of downstream collectors. Here, the intervention logic is not limited to road hardening. Additional intermediate shelters, neighborhood assembly points, staged evacuation protocols, and directional traffic management can reduce peak load concentration. In practical planning terms, these areas require operational measures that distribute demand in time and space, rather than relying solely on one final shelter destination. This is especially important where road widening is physically constrained by terrain or existing buildings.

The third category consists of receiving and transfer zones in relatively lower-exposure urban sectors that nevertheless function as bottleneck absorbers because multiple evacuation streams converge there. If these nodes are overlooked, improvements on upslope roads may simply shift congestion downstream. Therefore, shelter allocation, curb management, emergency signage, and intersection control in lower urban zones must be treated as part of the same evacuation system. The key policy implication is that priority areas for intervention are not identical to the highest hazard zones only; they are the places where hazard, route fragility, and concentrated future urban demand intersect most strongly.

Implications for Risk-Sensitive Spatial Planning in Ternate

The findings carry direct implications for spatial planning in Ternate because they show that the accumulation of evacuation risk is partly produced through ordinary development decisions. If built-up growth continues to move into slope-accessible but hazard-sensitive land without corresponding network enhancement, the island will not only contain more exposed assets; it will also contain more population that depends on fragile evacuation corridors. This means that risk-sensitive planning in Ternate should move beyond conventional hazard zoning toward a performance-based approach in which evacuation accessibility and bottleneck potential become explicit criteria in land-use regulation.

For the city's spatial planning instruments, including zoning and detailed development control, the results suggest that moderate and high bottleneck-growth zones should be treated as conditional development areas. In such areas, additional built-up expansion should be tied to measurable requirements, such as a minimum level of route redundancy, corridor improvement, slope drainage treatment, or provision of nearby shelters and assembly spaces. Areas that repeatedly exhibit high bottleneck scores across multiple scenarios should be prioritized for stricter control, especially where settlement expansion would intensify evacuation dependence on roads already exposed to lahar or landslide. In this respect, the study offers a more operational bridge between hazard maps and planning decisions.

The policy relevance also extends to infrastructure programming. Road investment on volcanic small islands is often justified by daily traffic demand alone, but the present results show that evacuation function should be incorporated into corridor prioritization. Short, strategically located links may provide more risk-reduction value than large but spatially disconnected projects. Likewise, shelter planning should not be based only on administrative coverage; it should respond to future accessibility loss, route convergence, and likely hazard-phase constraints. Such an approach is consistent with the wider literature on small volcanic islands, which highlights the difficulty of avoiding risk accumulation when land is scarce and development pressure remains strong (Komorowski et al., 2016; Wilkinson et al., 2016).

Finally, the Ternate-Gamalama case contributes to broader debates on volcanic and island planning by demonstrating that future evacuation bottlenecks are a tractable planning object. They can be modeled, mapped, compared across scenarios, and linked to concrete interventions. This makes them especially valuable for local governments that need analytically defensible priorities for corridor upgrading, shelter placement, and development control. The study therefore supports a shift from reactive evacuation mapping toward anticipatory evacuation governance, in which future growth patterns are assessed in relation to the carrying capacity of the emergency mobility system.

CONCLUSION

This study demonstrates that built-up land expansion on the slopes of Mount Gamalama is likely to intensify multi-hazard evacuation bottlenecks on Ternate Island between 2025 and 2055. The central mechanism is not urban growth in isolation, but the interaction between corridor-based settlement expansion, overlapping eruption-lahar-landslide exposure, and the limited redundancy of a volcanic small-island road network. The modeled results show a consistent increase in built-up land within hazard-sensitive areas, longer travel time to shelters, declining service-area coverage, and progressively higher bottleneck scores, especially on the west and northwest flanks and at key slope-to-coast transition nodes.

Scientifically, the paper contributes a unified framework that connects urban growth projection, multi-hazard overlay, and spatio-temporal evacuation network analysis. This addresses an important gap in the Ternate-Gamalama literature, where land-cover change, volcanic hazard, vulnerability, and evacuation have generally been studied in separate analytical streams. By explicitly identifying future bottleneck zones, the study advances geospatial disaster analysis from static exposure mapping toward dynamic evaluation of emergency accessibility under changing land-use conditions. The framework can be transferred to other compact volcanic islands by adapting local hazard layers, built-up growth drivers, road-network impedance parameters, shelter data, and population-demand scenarios to the relevant island context.

The study has several limitations. First, the built-up expansion scenarios represent a medium-growth trajectory based on historical land-cover transitions and do not fully capture sudden policy changes, major infrastructure investments, or informal settlement dynamics. Second, road capacity was represented using a functional-class proxy because detailed traffic counts, lane widths, and evacuation-mode shares were not consistently available for all segments. Third, the hazard-constrained evacuation model simplifies crisis-phase behavior and does not explicitly simulate household departure time, pedestrian evacuation, vehicle ownership, real-time traffic control, or dynamic shelter occupancy. These limitations indicate that the results should be interpreted as planning-oriented scenarios rather than deterministic forecasts. From a policy perspective, the findings support four main recommendations: strengthen control of new built-up development in recurrent bottleneck-growth zones; prioritize corridor upgrades and route diversification in west and northwest slope sectors; expand shelter and assembly-point provision in transition and receiving nodes; and incorporate evacuation performance indicators into spatial planning review. Future research should refine the model with higher-resolution traffic capacity data, household-level demand differentiation, dynamic shelter occupancy, and event-phase simulations that distinguish warning, peak disruption, and post-eruption lahar periods. Even in its current form, however, the framework offers a robust and operational basis for risk-sensitive spatial planning on Ternate Island.

AUTHOR CONTRIBUTIONS

MSM and DP were responsible for developing the study concept, defining the intellectual content, and serving as guarantors of the overall integrity of the manuscript. AP participated in the literature search, assisted with manuscript editing, and performed the final manuscript review.

CONFLICT OF INTEREST

The authors declare that they have no conflict of interest regarding the publication of this manuscript.

REFERENCES

Bonadonna, C., Frischknecht, C., Menoni, S., Romerio, F., Gregg, C. E., Rosi, M., Biass, S., Asgary, A., Pistolesi, M., Guobadia, D., Gattuso, A., Ricciardi, A., & Cristiani, C. (2021). Integrating hazard, exposure, vulnerability and resilience for risk and emergency management in a volcanic context: The ADVISE model. Journal of Applied Volcanology, 10, 7. https://doi.org/10.1186/s13617-021-00108-5

de Belizal, E., Lavigne, F., Hadmoko, D. S., Degeai, J.-P., Dipayana, G. A., Mutaqin, B. W., Marfai, M. A., Coquet, M., Le Mauff, B., Robin, A.-K., Vidal, C., Cholik, N., & Nurnaning, A. (2013). Rain-triggered lahars following the 2010 eruption of Merapi Volcano, Indonesia: A major risk. Journal of Volcanology and Geothermal Research, 261, 330-347. https://doi.org/10.1016/j.jvolgeores.2013.01.010

Ghosh, P., Mukhopadhyay, A., Chanda, A., Mondal, P., Akhand, A., Mukherjee, S., Nayak, S. K., Ghosh, S., Mitra, D., Ghosh, T., & Hazra, S. (2017). Application of cellular automata and Markov-chain model in geospatial environmental modeling: A review. Remote Sensing Applications: Society and Environment, 5, 64-77. https://doi.org/10.1016/j.rsase.2017.01.005

Hidayat, A., Marfai, M. A., & Hadmoko, D. S. (2020). Eruption hazard and challenges of volcanic crisis management on a small island: A case study on Ternate Island-Indonesia. International Journal of GEOMATE, 18(66), 171-178. https://doi.org/10.21660/2020.65.ICGEO43

Hidayat, A., Marfai, M. A., & Hadmoko, D. S. (2022). The 2015 eruption of Gamalama volcano (Ternate Island-Indonesia): Precursor, crisis management, and community response. GeoJournal, 87, 1-20. https://doi.org/10.1007/s10708-020-10237-w

Hidayat, A., Hadmoko, D. S., Marfai, M. A., et al. (2023). Volcanic hazard knowledge and preparedness of small island community on the flank of Gamalama volcano Ternate Island-Indonesia. GeoJournal, 88, 1251-1263. https://doi.org/10.1007/s10708-022-10682-9

Ikqra, Tjahjono, B., & Sunarti, E. (2012). Geomorphological study of Ternate Island and landslide hazard assessment. Jurnal Tanah Lingkungan, 14(1), 1-6.

Komorowski, J.-C., Morin, J., Jenkins, S., & Kelman, I. (2016). Challenges of volcanic crises on small islands states. In C. J. Fearnley, D. K. Bird, K. Haynes, W. J. McGuire, & G. Jolly (Eds.), Observing the Volcano World (pp. 353-371). Springer. https://doi.org/10.1007/11157_2015_15

Lessy, M. R., Lassa, J., & Zander, K. K. (2024). Understanding multi-hazard interactions and impacts on small-island communities: Insights from the active volcano island of Ternate, Indonesia. Sustainability, 16(16), 6894. https://doi.org/10.3390/su16166894

Lopez-Saavedra, M., & Marti, J. (2023). Reviewing the multi-hazard concept. Application to volcanic islands. Earth-Science Reviews, 236, 104286. https://doi.org/10.1016/j.earscirev.2022.104286

Mei, E. T. W., & Lavigne, F. (2012). Influence of the institutional and socio-economic context for responding to disasters: Case study of the 1994 and 2006 eruptions of the Merapi Volcano, Indonesia. Geological Society, London, Special Publications, 361(1), 171-186. https://doi.org/10.1144/SP361.14

Rampengan, M. M. F., Boedhihartono, A. K., Law, L., Gaillard, J. C., & Sayer, J. (2014). Capacities in facing natural hazards: A small island perspective. International Journal of Disaster Risk Science, 5(4), 247-264. https://doi.org/10.1007/s13753-014-0031-4

Rakuasa, H., & Khromykh, V. V. (2025). Spatio-temporal modeling of built-up land expansion (2005-2055) in the eruption prone area of Gamalama volcano, Ternate Island, Indonesia. Journal of Geospatial Science and Analytics, 1(3), 167-184. https://doi.org/10.58524/jgsa.v1i3.40

Sandri, L., Tierz, P., Costa, A., Marzocchi, W., & Garcia-Aristizabal, A. (2017). A framework for probabilistic multi-hazard assessment of rain-triggered lahars using Bayesian belief networks. Frontiers in Earth Science, 5, 73. https://doi.org/10.3389/feart.2017.00073

Sheladiya, K. P., & Patel, C. R. (2023). An application of Cellular Automata (CA) and Markov Chain (MC) model in urban growth prediction: A case of Surat City, Gujarat, India. Geoplanning: Journal of Geomatics and Planning, 10(1), 23-36. https://doi.org/10.14710/geoplanning.10.1.23-36

Syiko, S. F., Ayu, R. T., & Yudono, A. (2013). Evacuation route planning in Mount Gamalama, Ternate Island-Indonesia. Procedia Environmental Sciences, 17, 344-353. https://doi.org/10.1016/j.proenv.2013.02.047

Tsai, M.-T., & Chang, H.-W. (2023). Contribution of accessibility to urban resilience and evacuation planning using spatial analysis. International Journal of Environmental Research and Public Health, 20(4), 2913. https://doi.org/10.3390/ijerph20042913

White, R. (1998). Cities and cellular automata. Discrete Dynamics in Nature and Society, 2(2), 111-125. https://doi.org/10.1155/S1026022698000090

Wilkinson, E., Lovell, E., Carby, B., Barclay, J., & Robertson, R. E. A. (2016). The dilemmas of risk-sensitive development on a small volcanic island. Resources, 5(2), 21. https://doi.org/10.3390/resources5020021

Xu, T., Zhou, D., & Li, Y. (2022). Integrating ANNs and Cellular Automata-Markov Chain to simulate urban expansion with annual land use data. Land, 11(7), 1074. https://doi.org/10.3390/land11071074